Effects of Combustor Size and Filling Condition on Stability Limits of Premixed H_2-Air Flames in Planar Microcombustors

Jun Li, Yuantao Wang, Jinxing Chen, and Xueling Liu
Key Laboratory of Efficient Utilization of Low and Medium Grade Energy, Ministry of Education, Tianjin University, Tianjin 300072, P.R. China

Dept. of Energy and Power Engineering, School of Mechanical Engineering, Tianjin University, Tianjin 300072, P.R. China

Zhaoli Guo
State Key Laboratory of Coal Combustion, Huazhong University of Science and Technology, Wuhan 430074, P.R. China

DOI 10.1002/aic.14855
Published online May 7, 2015 in Wiley Online Library (wileyonlinelibrary.com)

An experimental study on stability limits of premixed hydrogen-air flames in planar microcombustors ($H = 1$ mm and 1.5 mm) partially filled with porous medium is carried out, focusing on the effects of combustor sizes and filling conditions. Critical conditions for blow-off, flashback, and breaking through the porous medium are experimentally measured. The blow-off limits are nearly independent of combustor sizes and filling conditions, while the flashback limits are strongly influenced by the combustor size and the filling conditions. Critical values for breaking through are identified with two different methods, and it is shown that standing combustion waves are settled over a range of velocities, instead of a fixed value of filtration velocity, which is considered an important characteristic of microcombustion. Most results can be explained by the classic boundary velocity gradient theory by von Elbe and Lewis, and thus the validity of the theory to the present channel spacings is confirmed. © 2015 American Institute of Chemical Engineers *AIChE J*, 61: 2571–2580, 2015

Keywords: hydrogen-air, premixed flames, stability limits, planar microcombustor, porous medium

Introduction

Ever since Epstein and Senturia[1] proposed the concept of the micro heat engines in 1997, various prototypes of miniaturized power systems, such as the micro gas turbine,[2] the micro-thermoelectric device,[3] the micro-thermophotovoltaic system,[4] and so on have been developed and tested, with a strong motivation enabled by the fact that hydrogen and many hydrocarbon fuels offer much higher energy densities than batteries, and thus miniaturizing the current power packages becomes feasible.[5] References [6–8] reviewed key progress in the research of microcombustion and the development of micro power systems. Despite the remarkable advances, it is pointed out that the understanding of fundamental flame behaviors and combustion characteristics in the microscale and mesoscale, for example, flame stabilities, is still insufficient.

Achieving stabilized flames in microcombustors is a challenging task due to the strong thermal coupling between the flame and combustor walls, which has been an important subject for microcombustion research. For this reason, methods like external heating,[9,10] backward-facing step,[11–13] catalyzed combustion,[14] heat recirculation,[15,16] and so on were employed. Among them, heat recirculation from the exhaust to the unburned mixture was shown to be effective in increasing the flame speed and extending flammability limits,[17,18] suggesting the importance of transporting heat from the "high temperature zone" to preheat the mixture in the case of microcombustion. Based on this principle, a planar microcombustor partially filled with porous medium was proposed in order to allow "internal" heat recirculation.[19] The microcombustor was fabricated and tested, and the results indicated that thermal radiation from the combustor wall could be greatly enhanced against the case without porous medium.[19,20] To better understand the dynamic behaviors of this specific configuration, critical conditions (mixture velocity U and equivalence ratio Φ) corresponding to flame stability limits for different combustor configurations were experimentally identified for an $H = 1$ mm microcombustor.[21] It was found that the blow-off limits are nearly independent of the combustor configuration, while the flashback limits are strongly influenced by the combustor configuration as well as the parameters of the inserted porous medium. As a follow-up, the present study is primarily intended to investigate the effects of the combustor size on the stability limits, and to provide a more in-depth analysis on the results.

Flame stability limits have been extensively studied for their theoretical importance and practical relevance to

Correspondence concerning this article should be addressed to J. Li at lijun79@tju.edu.cn.

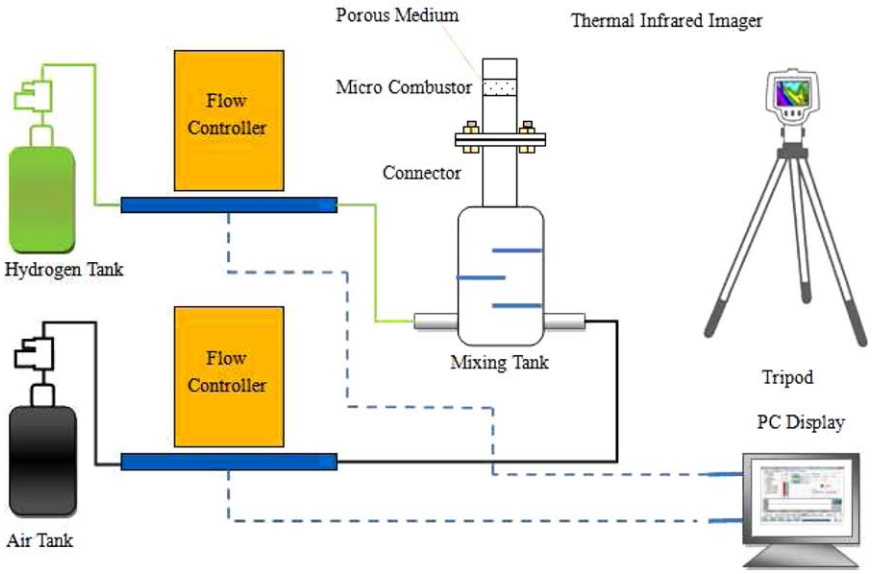

Figure 1. Schematic of the experimental setup.

[Color figure can be viewed in the online issue, which is available at wileyonlinelibrary.com.]

engineering applications. Back in 1949, von Elbe and Lewis[22] first presented the theory of flame stabilization by introducing the boundary velocity gradient near the combustor rim, based on which Putnam and Jensen[23] obtained the relations expressed in the form of dimensionless numbers (Peclet number). With a set of well-designed experimental apparatus, Grumer et al.[24] measured the flashback and blow-off limits of a wide range of fuels, and till today their results are still well valid for burner designs. However, when it comes to the near-quenching dimensions, heat losses which dictate thermal quenching become more significant, and the combustor material properties strongly affect the radical quenching.[10,25,26] Yuasa et al.[27] found that the boundary velocity gradient theory could not explain the experimental results when the tube diameter is smaller than 1 mm, but whether this critical dimension is a function of fuel types, equivalence ratios and other factors, remains unanswered. In fact, it was also pointed out by Grumer et al.[24] that the combustor size has a pronounced effect on the flame stability limits, especially the flashback conditions. For the reasons presented above, an experimental study is conducted to investigate the effects of combustor sizes and filling conditions on the flame stability limits, and by analyzing the experimental results to generalize some basic rules for the design and operation of this kind of microcombustors.

Experimental Setup and Approach

The experimental setup for the present study is schematically shown in Figure 1. It is exactly identical to what was used in an earlier study,[21] except that two microcombustors with $H = 1$ mm and 1.5 mm, respectively, are used. To avoid unnecessary repetition, details of the experimental setup are not given here.

The microcombustors are made of stainless steel (SS) 316L, and their design features and configurations are shown in Figure 2. The same aspect ratio (= 10) is used for both microcombustors in order to ensure that the majority of the flow to be two-dimensional. In the earlier study,[21] three configurations were tested: (a) without porous medium; (b) fully filled with porous medium; and (c) partially filled with porous medium, and it was found that it is very difficult to have flashbacks for (b). As such, only the configurations shown in Figures 2a, c are investigated in the present study. The distance from the upper boundary of the inserted porous medium to the combustor exit is denoted as L_{out} and the width of the porous medium as W, as illustrated in Figure 2, which are used to define the "filling conditions." The porous medium is made by folding the SS 316L mesh (wire diameter of ~0.229 mm and average pore diameter of ~0.28 mm) into multiple plies, with triple-ply and double-ply used for the H =1.5 mm and $H = 1$ mm microcombustors, respectively, to achieve the same porosity. Using the formula given in Ref. 21, the porosity of the porous medium is calculated to be 0.87. For more details about the fabrication of the porous medium and the calculation of the porosity, please refer to Ref. 21.

The fuel-air mixture is ignited by an external spark placed near the combustor exit. Under certain flow conditions (U and Φ), the flame propagates upstream back into the combustor. The outer walls of the planar microcombustor were oxidized very quickly (in less than an hour) once a stable flame was established inside. To ensure consistent wall properties, especially the thermal conductivity, the combustor was "burned" (having flame inside) for about 4 h prior to the experiment. Figure 3 illustrates the three critical conditions and they are defined as follows: (a) blow-off, under a given velocity U (superficial velocity based on the cross-sectional area of $H \times 10H$), there is a critical Φ, denoted as Φ_1 under which no flame can be established at the combustor rim; (b) flashback, under a given velocity U, there is a critical Φ, denoted as Φ_2 under which the flame can propagate back into the combustor and be stabilized somewhere inside the combustor; and (c) for the partially filled configuration, there is another critical Φ, denoted as Φ_3 above which the flame will break through the lower boundary of the porous medium, rendering the porous medium ineffective in "holding" the flame within it. It should be mentioned that Φ_1 and Φ_2 are applicable to all configurations in Figure 2, while Φ_3 is only applicable to Figure 2c.

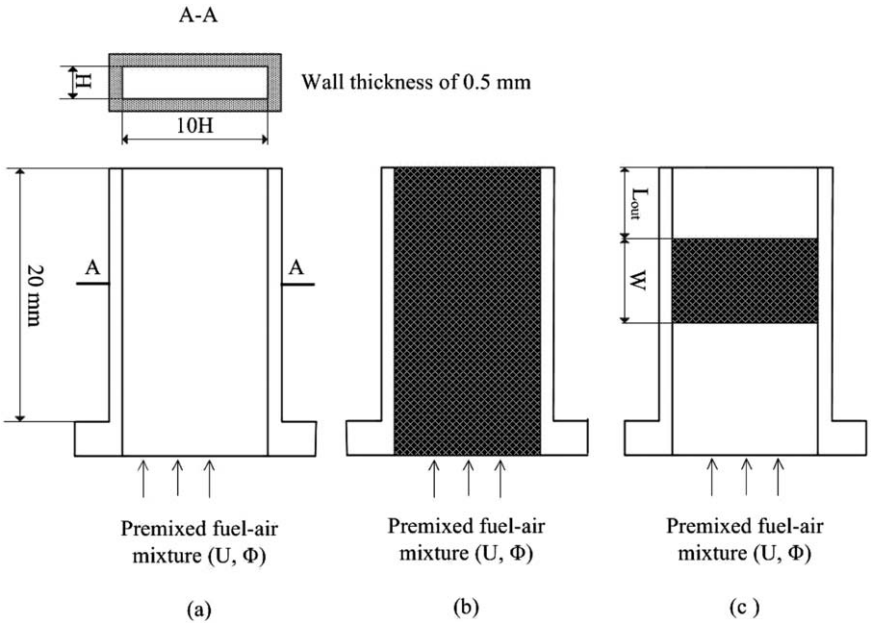

Figure 2. Design features and configurations of the planar microcombustors (not to scale).

The experimental procedure to identify the critical conditions for different combustor sizes and filling conditions is described as follows. Each time, a given flow velocity U is applied, and then a preliminary mixture equivalence ratio Φ is used for trial. Spark ignition is implemented after stable readings of the mass flow controllers are achieved. While fixing U, Φ is adjusted by an interval of 0.025 until a critical value is found. Due to the existence of flames (either at the combustor rim or inside the combustor), the combustor walls are heated to a higher temperature than the ambient, which can be readily detected by the infrared thermal imager. Upon each trial, an air blower is used to cool down the combustor until the external wall temperature approaches 25°C—this is to ensure the thermal boundary conditions to be consistent throughout the experiment. The procedure described above is applicable to both Φ_1 and Φ_2, as schematically shown in Figure 4, while for Φ_3, the case is a bit more complicated, and its procedure is detailed in Critical conditions for flames breaking through the porous medium section. Each value of the critical equivalence ratio (Φ_1, Φ_2, and Φ_3) is finalized only after the result is repeated at least twice under the identical conditions. The experimental error of Φ is about 1.4%, and therefore, error bars are not shown in the following figures due to their smaller sizes compared to those of the symbols.[21]

Results and Discussion

The velocity range for the present study is determined to be $U = 1$–3 m/s. $U < 1$ m/s does not generate sufficient thermal energy for practical micro power systems, while the upper limit ($U = 3$ m/s) is chosen out of consideration that a

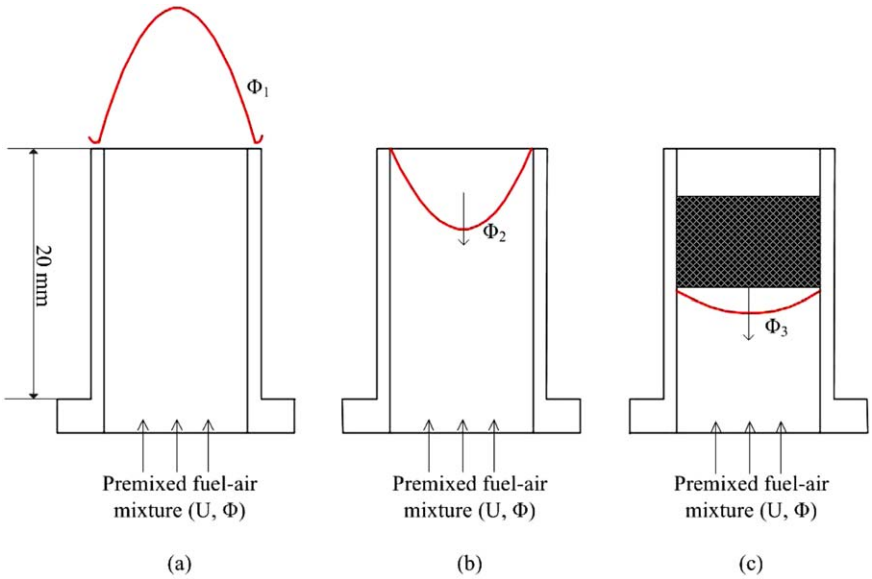

Figure 3. Illustration of the three critical conditions.

[Color figure can be viewed in the online issue, which is available at wileyonlinelibrary.com.]

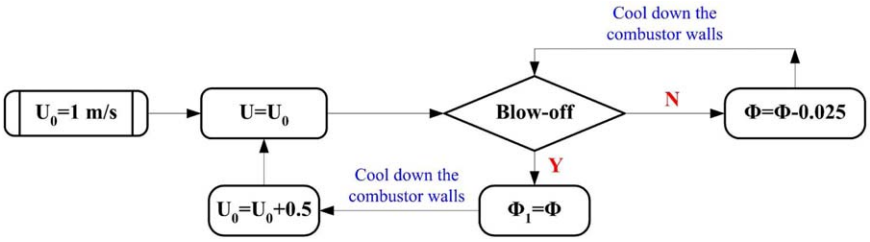

(a) Φ_1 for blow-off

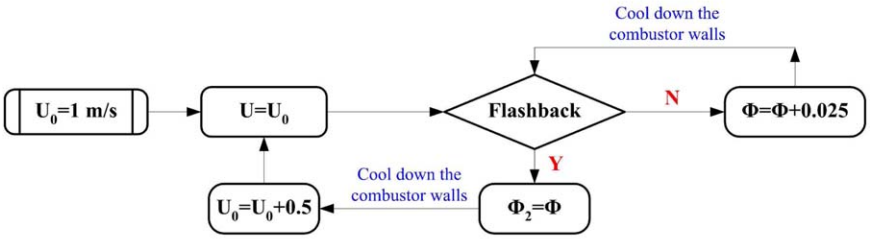

(b) Φ_2 for flashback

Figure 4. Flowcharts of the experimental procedure for Φ_1 and Φ_2. (a) Φ_1 for blow-off; (b) Φ_2 for flashback.

[Color figure can be viewed in the online issue, which is available at wileyonlinelibrary.com.]

higher velocity may result in burnout of the inserted porous medium. To study the effects of filling conditions, there are totally six filling conditions designed for each microcombustor. The grouping of the experimental cases is given in Table 1.

Critical conditions for blow-off

The results of the critical conditions for blow-off are given in Table 2. It can be seen that within the velocity range, the critical equivalence ratios (Φ_1) do not differ significantly among the experimental cases given in Table 1. In other words, Φ_1 can be taken as 0.3 (± 0.05) when $1 \leq U \leq 3$ m/s. To compare the above results with those obtained by von Elbe and Lewis[22] and Grumer et al.,[24] the velocity gradient at the exit of the microcombustor needs to be known. However, this is very difficult to get. From Figure 1, it can be seen that the flow velocity at the combustor inlet is almost uniform. Using a simple empirical relation[28] $L_h \approx 0.05Re \times D$ to estimate the hydrodynamic entrance length, one obtains: for $H = 1$ mm, L_h is around 13, 28, and 39 mm for $U = 1$, 2, 3 m/s, respectively; and for $H = 1.5$ mm, L_h is around 29, 57, and 86 mm for $U = 1$, 2, 3 m/s, respectively. Take note that $D = 2H$ and the viscosity of air at 300 K are used in the above calculation. The results of L_h indicate that the flow velocity has not reached the fully developed condition for most cases, as the combustor length is only 20 mm (see Figure 2). Therefore, a quantitative comparison is unfeasible, and the data presented in Table 2 are only examined in a qualitative manner. It was pointed out in Ref. 24 that blow-off gradients are less affected by tube diameters near quenching dimensions. In addition, Fig. 25 of Ref. 24 (titled "Flame stability diagram for fuel hydrogen") shows that when $\Phi < 0.4$, the blow-off curve becomes very steep, implying that blow-off happens over a considerably wide range of velocity gradients when the mixture is lean to 0.4 and below, which is considered to be in some qualitative agreement with the experimental results given in Table 2. Based on the limited cases tested in the present study, it is concluded that the blow-off limits are mainly determined by the mixture composition. Φ_1 increases very insignificantly with the increase of the flow velocity, and is almost independent of combustor sizes and filling conditions, especially at higher flow velocities.

Table 1. Grouping of the Experimental Cases

Description of Cases		
$H = 1$ mm	$H = 1.5$ mm	Purpose
(1) Without porous medium, Figure 2a (2) [a]$W = 5$ mm, $L_{out} = 7$ mm, Figure 2c		Effects of inserted porous medium
(3) $W = 3$ mm, $L_{out} = 7$ mm, Figure 2c (2) [a]$W = 5$ mm, $L_{out} = 7$ mm, Figure 2c (4) $W = 10$ mm, $L_{out} = 7$ mm, Figure 2c		Effects of the width of the porous medium
(5) $W = 5$ mm, $L_{out} = 3$ mm, Figure 2c (2) [a]$W = 5$ mm, $L_{out} = 7$ mm, Figure 2c (6) $W = 5$ mm, $L_{out} = 14$ mm, Figure 2c		Effects of the distance from the porous medium upper boundary to the combustor exit

[a]Reference case.

Table 2. Critical Equivalence Ratios (Φ_1) for Blow-Off

		U									
		1 m/s		1.5 m/s		2 m/s		2.5 m/s		3 m/s	
		H									
Description of Cases		1 mm	1.5 mm	1 mm	1.5 mm	1 mm	1.5 mm	1 mm	1.5 mm	1 mm	1.5 mm
Without porous medium	Φ_1	0.3	0.3	0.3	0.325	0.325	0.325	0.325	0.35	0.35	0.35
$W = 3$ mm, $L_{out} = 7$ mm		0.325	0.325	0.325	0.325	0.325	0.35	0.35	0.35	0.35	0.35
$W = 5$ mm, $L_{out} = 7$ mm		0.3	0.3	0.3	0.3	0.325	0.325	0.325	0.35	0.35	0.35
$W = 10$ mm, $L_{out} = 7$ mm		0.3	0.325	0.3	0.325	0.35	0.35	0.35	0.35	0.35	0.35
$W = 5$ mm, $L_{out} = 3$ mm		0.3	0.3	0.3	0.325	0.325	0.35	0.35	0.35	0.35	0.35
$W = 5$ mm, $L_{out} = 14$ mm		0.275	0.3	0.3	0.325	0.325	0.35	0.35	0.35	0.35	0.35

Critical conditions for flashback

Figure 5 shows the comparison of the critical equivalence ratio (Φ_2) between "without porous medium" and "partially filled with porous medium." First, the overall trend is that Φ_2 increases with the increasing velocity, which is similar to the results of natural gas flames given by von Elbe and Lewis.[22] Second, it is also shown that Φ_2 can be considerably lowered by partially filling the microcombustor with porous medium. Following the velocity gradient theory, for the two configurations in Figures 2a, c, one can easily have $G_a > G_c$ (G representing the velocity gradient), thus leading to $\Phi_{2,a} > \Phi_{2,c}$. Third, Figure 5 indicates that the larger combustor requires a smaller Φ_2 for the flame to flashback. In Grumer et al.'s experimental study,[24] the smallest tube diameter used for hydrogen-air is 2.3 mm, and no size effects were observed in the G-Φ diagram (Fig. 25 of Ref. 24). In the present study, the characteristic lengths are about 2 mm and 3 mm (hydraulic diameter = $2H$), very close to 2.3 mm. Based on the above argument, it is believed that the difference in terms of Φ_2 between the two combustor sizes is attributed more to the velocity gradient, a parameter not being able to be quantified in the present study, than the surface-to-volume ratio (nearly proportional to H^{-1}) which has a profound effect on heat losses.

The effects of filling conditions, they are, L_{out} and W, are illustrated in Figure 6. The overall trend is that with the increase of U, Φ_2 increases accordingly. The results for $H = 1$ mm have been reported and analyzed in Ref. 21, and the same analysis can be applied to explain the effects of L_{out} and W for the $H = 1.5$ mm microcombustor as well. With regards to the combustor size effects, it is consistent that for all cases in Figure 6, the larger combustor gives a lower Φ_2. Again, this is believed to be a result of the velocity gradient.

In Putnam and Jensen's analysis,[23] a condition was defined as "partial flame speed relation," referring to the case of near-quenching dimensions when the tube is too

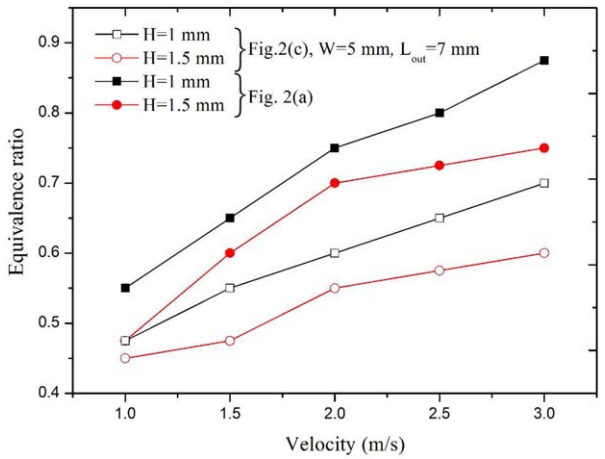

Figure 5. Effects of the inserted porous medium on flashback limits (Φ_2).

[Color figure can be viewed in the online issue, which is available at wileyonlinelibrary.com.]

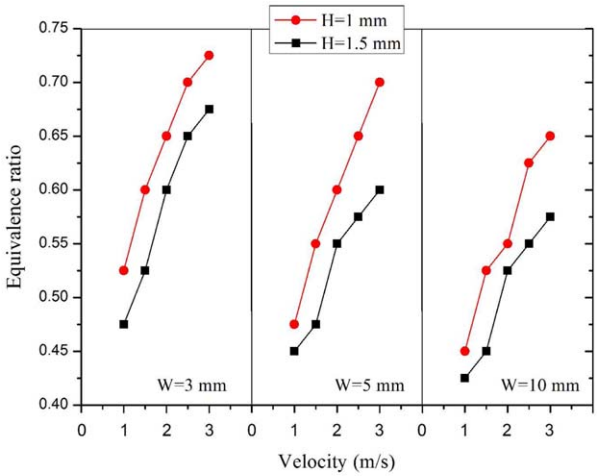

(a) Effects of W (L_{out}=7 mm)

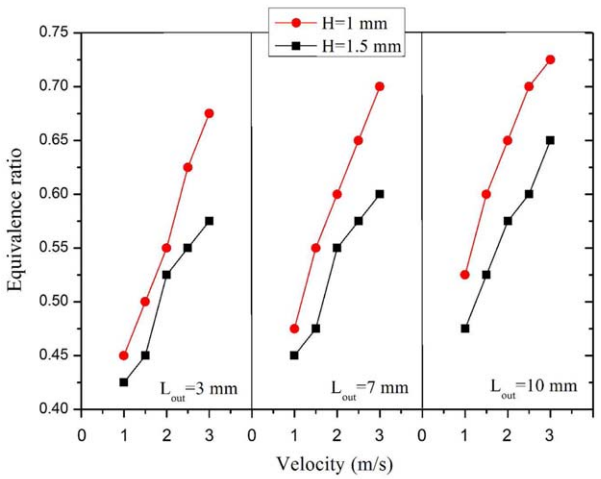

(b) Effects of L_{out} (W=5 mm)

Figure 6. Results of the flashback limits (Φ_2). (a) Effects of W ($L_{out} = 7$ mm). (b) Effects of L_{out} ($W = 5$ mm).

[Color figure can be viewed in the online issue, which is available at wileyonlinelibrary.com.]

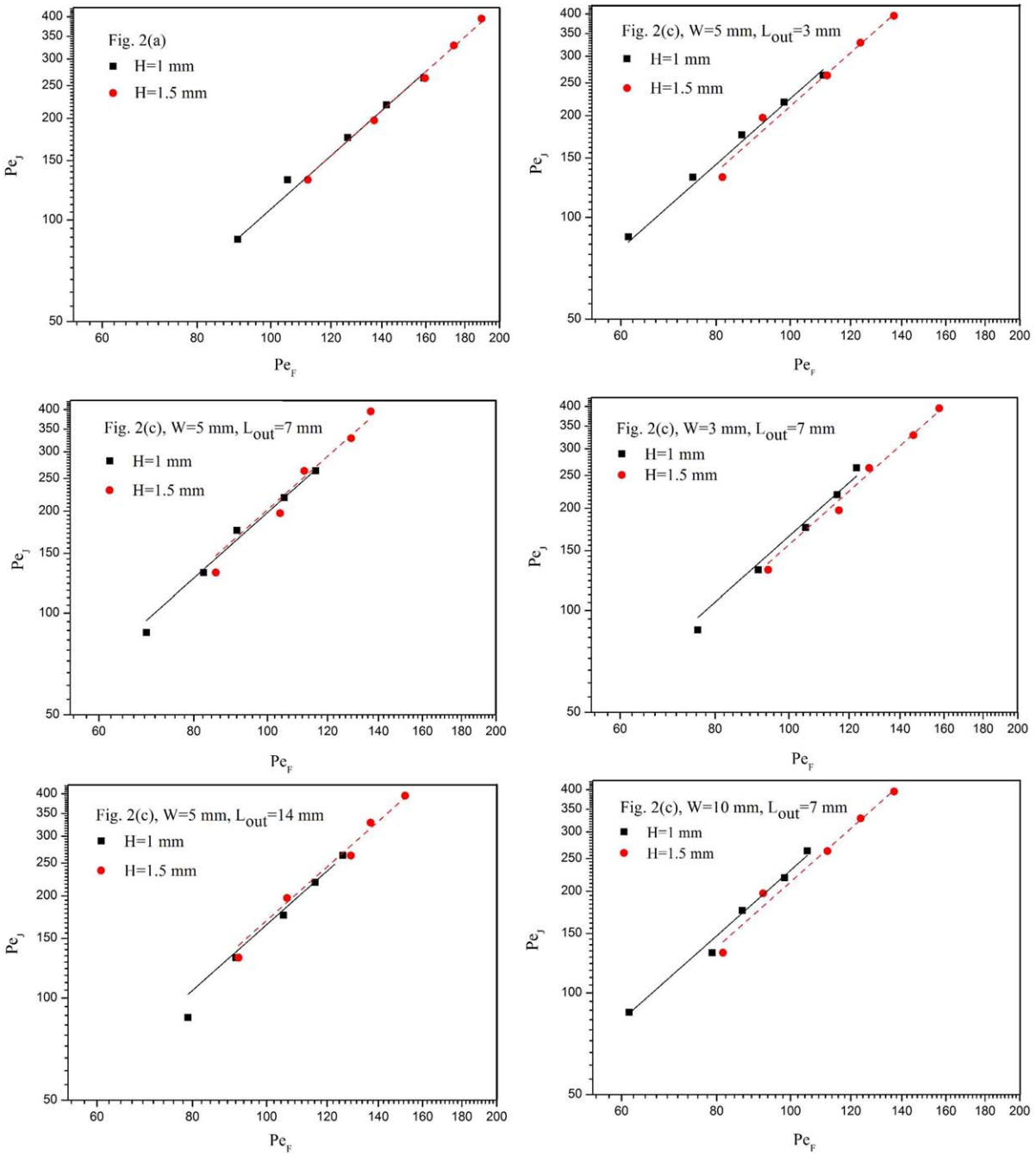

Figure 7. Representation of flashback limits (Φ_2) under different filling conditions.

[Color figure can be viewed in the online issue, which is available at wileyonlinelibrary.com.]

small for the flame speed to reach the free propagating speed for a given equivalence ratio. For the combustor dimensions examined in this study, the "partial flame speed relation" is unlikely to happen, and therefore, the boundary velocity gradient theory is believed still valid. With this assumption, Putnam and Jensen[23] correlated two dimensionless numbers, Pe_F and Pe_J, for flashback limits in the form as follows

$$Pe_J = C\,Pe_F{}^2 \tag{1}$$

where Pe_F is the Peclet number based on the flame speed S_L, Pe_J is the Peclet number based on the average jet velocity U, and C a constant independent of tube diameters. Their expressions are given as follows

$$Pe_F = \frac{2RS_Lc_p\rho}{\lambda},\ Pe_J = \frac{2RUc_p\rho}{\lambda} \tag{2}$$

With Eqs. 1 and 2, using the air properties, substituting R with H, and taking the values of S_L under different equivalence ratios from Ref. 29, the results in Figures 5 and 6 can be replotted in the logarithmic scales, as shown in Figure 7. Second-order polynomial fitting is employed for the data points, and the fitting results are summarized in Table 3.

Table 3. Results of Data Fitting for Φ_2

	C		Standard Error (10^{-4})		Relative Error (%)
	H				
Filling Conditions	1 mm	1.5 mm	1 mm	1.5 mm	$\frac{\lvert C_1-C_{1.5}\rvert}{\min\{C_1,C_{1.5}\}}$
Without medium	0.01077	0.01075	2.05749	1.30716	0.186
$W = 3$ mm, $L_{out} = 7$ mm	0.01650	0.01591	3.72601	2.40710	3.701
$W = 5$ mm, $L_{out} = 7$ mm	0.01981	0.02018	3.21488	5.43659	1.867
$W = 10$ mm, $L_{out} = 7$ mm	0.02307	0.02131	4.1780	3.4953	8.256
$W = 5$ mm, $L_{out} = 3$ mm	0.02244	0.02131	4.20930	3.48530	5.302
$W = 5$ mm, $L_{out} = 14$ mm	0.01645	0.01693	4.52717	3.50152	2.917

From Eq. 1, one obtains: $\lg Pe_J = \lg C + 2\lg Pe_F$, which shows that the fitted lines have the slope of 2 and the intercept of $\lg C$. Each graph of Figure 7 represents a specific filling condition (a combination of L_{out} and W) for two combustor dimensions. It can be seen that the slopes of two fitted lines are almost identical (= 2), indicating that Eq. 1 is well valid. In addition, the results given in Table 3 suggest that the constant C is almost independent of the channel spacing H. Based on this finding, the results of Figure 7 are collated in Figure 8 for the $H = 1$ mm microcombustor to better understand the effects of filling conditions on the constant C in Eq. 1. It is shown that when L_{out} is fixed, increasing W results in a larger intercept; when W is fixed, increasing L_{out} leads to a smaller intercept. In both Figures 8a, b, the no-filling condition gives the smallest intercept, and the closer the filling condition is to the no-filling case, the smaller the intercept.

If the constant C is independent of the combustor size, then it can be derived from Eq. 1 to have the following relation

$$S_{L,1} = \sqrt{\frac{H_2}{H_1}\frac{\alpha_1}{\alpha_2}}\,S_{L,2} \tag{3}$$

where the subscripts 1 and 2 refer to the two combustor dimensions, and α the thermal diffusivity. Assuming $\alpha_1/\alpha_2 = 1$, one can obtain that when the channel spacing H is reduced from 1.5 to 1 mm, the critical flame speed corresponding to flashback limits is decreased by a factor of $(1/1.5)^{0.5} \approx 0.8$, meaning that S_L is lowered by about 20%, and consequently a lower Φ_2, as shown in Figure 6. A potential application of Eq. 3 is that once the flashback limits are known for one combustor size, one can easily derive the flashback limits for another size.

Critical conditions for flames breaking through the porous medium

In the earlier study,[21] it was found that when applying an equivalence ratio Φ greater than the flashback limit ($\Phi > \Phi_2$), there are two possibilities: (1) the flame is stabilized within the porous medium; and (2) above a certain Φ, denoted as Φ_3, the flame breaks through the lower boundary of the porous medium and eventually is stabilized at the inlet. However, under certain filling conditions, (2) happens when $\Phi = \Phi_2$, meaning that once the flame propagates into the combustor, it straight away breaks through the porous medium (sometimes with retardation of a few seconds). For example, for the $H = 1$ mm combustor under the filling conditions of $L_{out} = 7$ mm and $W = 5$ mm, Figure 6 shows that $\Phi_2 = 0.65$ for $U = 2.5$ m/s. In our experiment, when $\Phi = 0.65$ is used, what happens is that upon flashback, the flame enters the porous medium, heating it up, and after a few seconds it breaks through the lower boundary of the porous medium. In that particular situation, Φ_2 and Φ_3 merges, but we could not tell what a lower Φ will result in because it could not overcome the flashback limit (Φ_2) at the exit. For this reason, a "bypassing" method is employed. For the same example filling condition mentioned above, the following steps are implemented to obtain Φ_3. First, set the flow velocity $U = 1.5$ m/s ($\Phi_2 = 0.55$, $\Phi_3 = 0.675$), and $\Phi = 0.6$ ($\Phi_2 < \Phi < \Phi_3$) is used. Then, ignite the mixture and

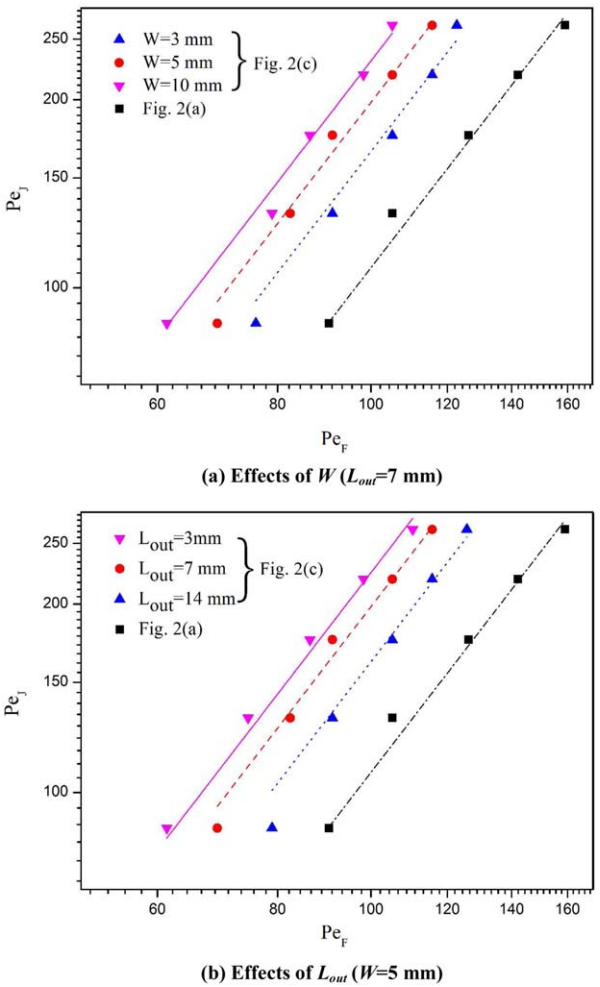

Figure 8. Effects of filling conditions on the constant C in Eq. 1. (a) Effects of W ($L_{out} = 7$ mm). (b) Effects of L_{out} ($W = 5$ mm).

[Color figure can be viewed in the online issue, which is available at wileyonlinelibrary.com.]

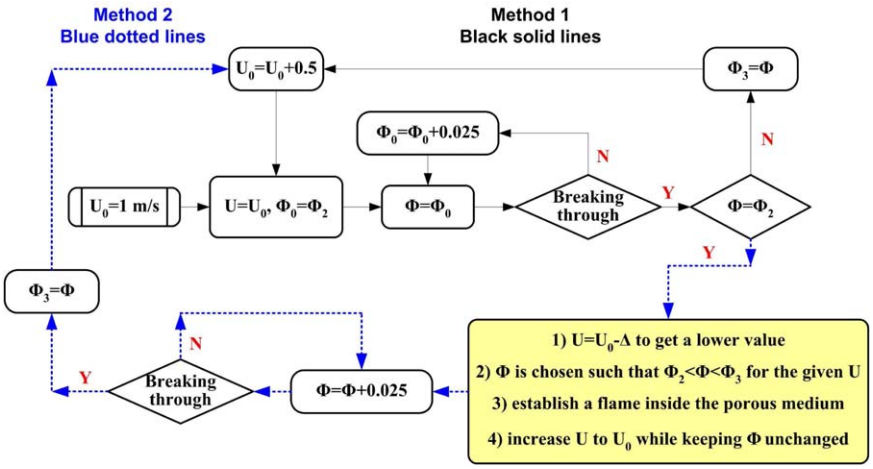

Figure 9. Flowchart of the experimental procedure for Φ_3.

[Color figure can be viewed in the online issue, which is available at wileyonlinelibrary.com.]

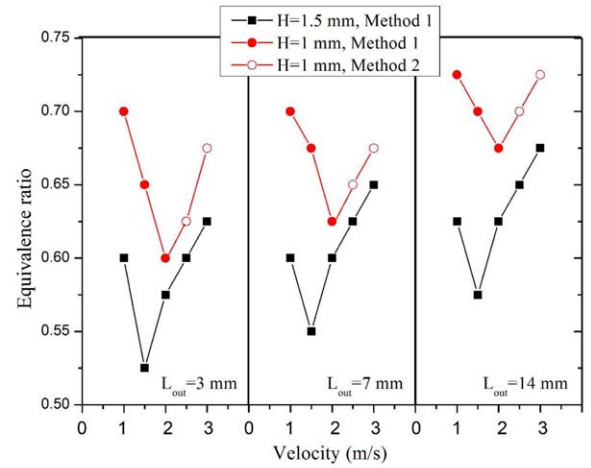

(a) Effects of L_{out} (W=5 mm)

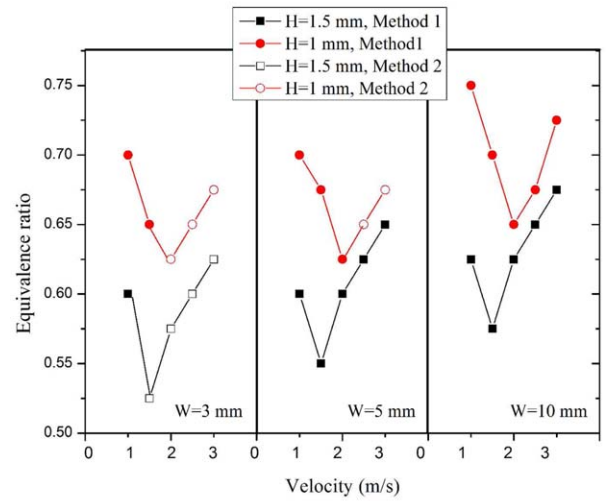

(b) Effects of W (L_{out}=7 mm)

Figure 10. Results of critical conditions for breaking through (Φ_3). (a) Effects of L_{out} ($W = 5$ mm). (b) Effects of W ($L_{out} = 7$ mm).

[Color figure can be viewed in the online issue, which is available at wileyonlinelibrary.com.]

a flame is established inside the porous medium. Next, U is increased to 2.5 m/s (the desired value) by keeping $\Phi = 0.6$ unchanged, and now the stable flame is still inside the porous medium. Finally, increase Φ from 0.6 by an interval of 0.025 while carefully observing the change of the flame position. The critical value for Φ_3 is recorded when flame breaking through the porous medium occurs. The process described above, named "Method 2," is illustrated in Figure 9 in blue dotted lines, while the normal procedure, named "Method 1," in black solid lines. It should be pointed out that "breaking through" happens under the "hot wall" condition, and therefore, cooling down the combustor walls (Figure 4) is not necessary any more in the measurement of Φ_3. For both Method 1 and Method 2, values of Φ_3 are recorded after the flame being stabilized inside the porous medium for at least 5 min.

Using the procedure illustrated in Figure 9, the results of Φ_3 are obtained, and are shown in Figure 10. It is consistent for all filling conditions that the larger combustor gives a lower value of Φ_3, suggesting that a smaller combustor is able to "withstand" a higher flame speed, in which heat losses through the external combustor walls are believed to play an important role. As the combustor size shrinks, the surface-to-volume ratio increases, and the net result is that the ratio of heat losses to heat generation increases. As such, in order to sustain the same flow velocity inside the porous medium, a smaller combustor requires a larger equivalence ratio to compensate for its higher heat losses. This finding, the authors believe, could be a very important characteristic associated with the small combustor sizes, and does not exist in large-scale porous medium combustors.

Application of the critical conditions

Flame stability limits are of great theoretical importance to combustion science and practical relevance to engineering applications, for example, burner designs. Having discussed the results and implications of Φ_1, Φ_2, and Φ_3 separately, it is useful to put them in a composite diagram in order to provide directions for designs and operation of the partially filled microcombustor, and an example case ($W = 5$ mm, $L_{out} = 7$ mm) is done in Figure 11. It is seen that the Φ-U diagram is divided into two regions, namely, Region 1 and Region 2. A point (U and Φ) taken from Region 2 will lead

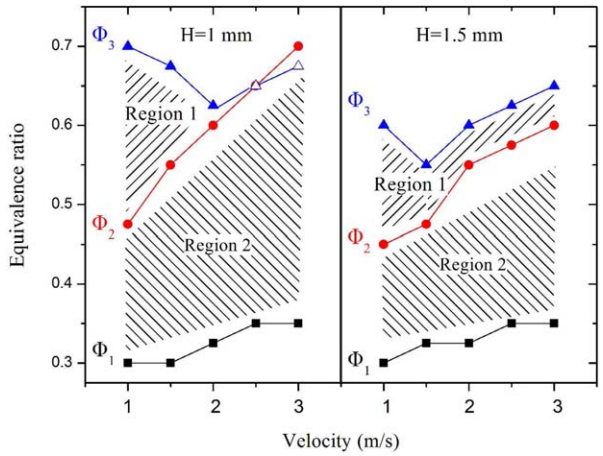

Figure 11. Composite diagram of flame stability limits ($W = 5$ mm, $L_{out} = 7$ mm).

[Color figure can be viewed in the online issue, which is available at wileyonlinelibrary.com.]

to a Bunsen-burner-typed flame sitting at the exit of the microcombustor, while a point taken from Region 1 gives a stable flame within the porous medium. However, it is noticed that Region 1 shrinks to almost zero for $H = 1$ mm when $U > 1.5$ m/s, but this does not mean that no stable flames can be established within the porous medium when $U > 1.5$ m/s. Recalling the "bypassing" method described in Critical conditions for flames breaking through the porous medium section and illustrated in Figure 10, an easy and simple strategy is to pick a point from Region 1 (<1.5 m/s) to set up a flame in the porous medium first, and gradually adjust the flow rates of air and hydrogen to the desired value of U, which is essentially a measure to change the thermal boundary condition of the combustor walls. Similar diagrams can be obtained for other filling conditions, based on which ignition and operation strategy for the particular configuration can be easily determined and implemented in combustor designs.

It is also found in Figure 11 that the inserted porous medium allows standing combustion waves over a range of velocities, instead of a fixed value, under a certain Φ. A similar finding was also reported by Yang et al.[30] and Fursenko et al.[31] for methane-air flames in high-porosity microfibrous porous media. Again, it is believed that the ability of sustaining standing combustion waves in the porous medium over a wider range of velocities and equivalence ratios than large-scale counterparts is attributed to the small combustor sizes. Supposing a standing combustion wave is established under a certain combination of U and Φ, increasing the velocity by ΔU would push the wave downstream and finally blow it off from the porous medium in large-scale combustors. However, in the scenario of microcombustion, ΔU also means a higher flame temperature, which is not the case in large-scale combustors. The increased flame temperature in turn gives rise to a higher flame speed, and consequently a new balance is achieved under $U+\Delta U$. Although this is a rather course analysis based on a quasi-one-dimensional assumption, it illustrates the essential mechanism of flame stabilization inside the porous medium in microcombustors. Further studies are underway to reveal the underlying mechanism in a more quantitative way.

Conclusion

An experimental study on the flame stability limits of premixed hydrogen-air combustion in planar microcombustors (spacings of $H = 1$ mm and 1.5 mm) partially filled with porous medium is carried out in order to investigate the effects of combustor sizes and filling conditions. Critical conditions for blow-offs (Φ_1), flashbacks (Φ_2), and breaking through the porous medium (Φ_3) were experimentally measured. The results of Φ_1 indicate that the blow-off limits are almost independent of combustor sizes and filling conditions. However, the flashback limits are strongly influenced by the combustor size and the filling condition defined by the position (L_{out}) and the width (W) of the inserted porous medium. Critical values for Φ_3 are identified with two different methods, and it is shown that standing combustion waves are sustained over a range of velocities, instead of a fixed value of filtration velocity, which is considered an inherent and important characteristic of microcombustion. Most of the experimental results can be explained by the classic boundary velocity gradient theory by von Elbe and Lewis, and thus the validity of the theory to the present channel spacings is confirmed.

Acknowledgments

The authors gratefully acknowledge the financial support provided by the National Natural Science Foundation of China (Grant No. 51306129). The work is also partly funded by the Foundation of State Key Laboratory of Coal Combustion (Project No. FSKLCC1411).

Literature Cited

1. Epstein AH, Senturia D. Macro power from micro machinery. *Science*. 1997;276:1211.
2. Waitz IA, Gauba G, Yang ST. Combustors for micro-gas turbine engines. *ASME J Fluids Eng*. 1998;120:109–117.
3. Sitzki L, Borer K, Schuster E, Ronney PD, Wussow S. Microscale combustion research for applications to MEMS rotary IC engine. In: *The 3rd Asia-Pacific Conference on Combustion*. Seoul, Korea, 2001.
4. Yang WM, Chou SK, Shu C, Li ZW, Xue H. Development of micro thermophotovoltaic system. *Appl Phys Lett*. 2002;81:5255–5257.
5. Ohadi MM, Buckley SG. High temperature heat exchangers and microscale combustion systems: applications to thermal system miniaturization. *Exp Therm Fluid Sci*. 2001;25:207–217.
6. Ju Y, Maruta K. Microscale combustion: technology development and fundamental research. *Prog Energy Combust Sci*. 2011;37:669–715.
7. Walther DC, Ahn J. Advances and challenges in the development of power-generation systems. *Prog Energy Combust Sci*. 2011;37:583–610.
8. Kaisare NS, Vlachos DG. A review on microcombustion: fundamentals, devices and applications. *Prog Energy Combust Sci*. 2012;38:321–359.
9. Maruta K, Kataoka T, Kim NI, Minaev S, Fursenko R. Characteristics of combustion in a narrow channel with a temperature gradient. *Proc Combust Inst*. 2005;30:2429–2436.
10. Prakash S, Armijo AD, Masel RI, Shannon MA. Flame dynamics and structure within sub-millimeter combustors. *AIChE J*. 2007;53:1568–1577.
11. Yang WM, Chou SK, Shu C, Li ZW, Xue H. Combustion in micro-cylindrical combustors with and without a backward facing step. *Appl Therm Eng*. 2002;22:1777–1787.
12. Li J, Chou SK, Huang G, Yang WM, Li ZW. Study on premixed combustion in cylindrical micro combustors: transient flame behavior and wall heat flux. *Exp Therm Fluid Sci*. 2009;33:764–773.
13. Li J, Chou SK, Li ZW, Yang WM. Characterization of wall temperature and radiation power through cylindrical dump micro-combustors. *Combust Flame*. 2009;156:1587–1593.
14. Boyarko GA, Sung C, Schneider SJ. Catalyzed combustion of hydrogen-oxygen in platinum tubes for micro-propulsion applications. *Proc Combust Inst*. 2005;30:2481–2488.

15. Kim NI, Kato S, Kataoka T, Yokomori T, Maruyama S, Fujimori T, Maruta K. Flame stabilization and emission of small Swiss-roll combustors as heaters. *Combust Flame*. 2005;141:229–240.
16. Lee KH, Kwon OC. Studies on a heat-recirculating micro emitter for a micro thermophotovoltaic system. *Combust Flame*. 2008;153:161–172.
17. Ju Y, Choi CW. An analysis of sub-limit flame dynamics using opposite propagating flames in mesoscale channels. *Combust Flame*. 2003;133:483–493.
18. Ronney PD. Analysis of non-adiabatic heat-recirculating combustors. *Combust Flame*. 2003;135:421–439.
19. Li J, Chou SK, Li ZW, Yang WM. A potential heat source for the micro thermophotovoltaic (TPV) System. *Chem Eng Sci*. 2009;64: 3282–3289.
20. Li J, Chou SK, Li ZW, Yang WM. Experimental investigation of porous media combustion in a planar micro-combustor. *Fuel*. 2010; 89:708–715.
21. Li J, Wang Y, Shi J, Liu X. Dynamic behaviors of premixed hydrogen-air flames in a planar micro-combustor filled with porous medium. *Fuel*. 2015;145:70–78.
22. von Elbe G, Lewis B. Theory of ignition, quenching and stabilization of flames of non-turbulent gas mixtures. In: *The Third Symposium (International) on Combustion and Flame and Explosion Phenomena*. Baltimore, MD: Williams & Wilkins, 1948:68–79.
23. Putnam AA, Jensen RA. Application of dimensionless numbers to flash-back and other combustion phenomena. In: *The Third Symposium (International) on Combustion and Flame and Explosion Phenomena*. Baltimore, MD: Williams & Wilkins, 1948:89–98.
24. Grumer J, Harris ME, Rowe VR. *Fundamental Flashback, Blowoff, and Yellow-Tip Limits of Fuel Gas-Air Mixtures*. Report of Investigation 5225, Pittsburgh, PA: Bureau of Mines, 1956.
25. Miesse CM, Masel RI, Jensen CD, Shannon MA, Short M. Submillimeter-scale combustion. *AIChE J*. 2004;50:3206–3214.
26. Miesse CM, Masel RI, Short M, Shannon MA. Experimental observations of methane-oxygen diffusion flame structure in a submillimeter microburner. *Combust Theory Model*. 2005;9:77–92.
27. Yuasa S, Oshimi K, Nose H, Tennichi Y. Concept and combustion characteristics of ultra-micro combustors with premixed flame. *Proc Combust Inst*. 2005;30:2455–2462.
28. Çengel YA, Cimbala JM. *Fluid Mechanics: Fundamentals and Applications, 2nd ed*. New York: McGraw Hill, Inc., 2010.
29. Liu DDS, MacFarlane R. Laminar burning velocities of hydrogen-air and hydrogen-air-steam flames. *Combust Flame*. 1983;49:59–71.
30. Yang HL, Minaev S, Geynce E, Nakamura H, Maruta K. Filtration combustion of methane in high-porosity micro-fibrous media. *Combust Sci Technol*. 2009;181:1–16.
31. Fursenko R, Minaev S, Maruta K, Nakamura H, Yang H. Characteristic regimes of premixed gas combustion in high-porosity micro-fibrous porous media. *Combust Theory Model*. 2010;14:571–581.

Manuscript received Jan. 14, 2015, and revision received Mar. 19, 2015.